

See discussions, stats, and author profiles for this publication at: <https://www.researchgate.net/publication/230866197>

Femtosecond Emission Studies on Gold Nanoparticles

ARTICLE *in* THE JOURNAL OF PHYSICAL CHEMISTRY B · AUGUST 2002

Impact Factor: 3.3 · DOI: 10.1021/jp020656+

CITATIONS

31

READS

43

8 AUTHORS, INCLUDING:



Dae Hong Jeong

Seoul National University

132 PUBLICATIONS **3,528** CITATIONS

SEE PROFILE



Dongho Kim

Yonsei University

502 PUBLICATIONS **13,533** CITATIONS

SEE PROFILE



Gyoujin Cho

Sunchon National University

87 PUBLICATIONS **2,149** CITATIONS

SEE PROFILE

Femtosecond Emission Studies on Gold Nanoparticles

Young-Nam Hwang, Dae Hong Jeong, Hyun Jong Shin, and Dongho Kim*

National Creative Research Initiatives Center for Ultrafast Optical Characteristics Control and Department of Chemistry, Yonsei University, Seoul 120-749, Korea

Sae Chae Jeoung

Laser Metrology Laboratory, Korea Research Institute of Standards and Science, Taejeon 305-600, Korea

Seon Hee Han and Jae-Suk Lee

Department of Materials and Engineering, Kwangju Institute of Science and Technology, Kwangju 500-712, Korea

Gyoujin Cho

Department of Chemical Engineering, Sunchon National University, 315 Maegok, Suncheon, Chonnam 540-742, Korea

Received: March 7, 2002; In Final Form: May 24, 2002

We report the light emission decay in bare gold nanoparticles by using the fluorescence up-conversion technique. The emission decay, of which the time constants increase consistently with excitation intensity, closely follows the electron thermalization dynamics, which has been independently observed from the bleach recovery of the surface plasmon band under the identical experimental conditions. These results indicate that a weak light emission from relatively large gold nanoparticles is attributable to the interactions between surface plasmons and incident photons, which occur simultaneously with the thermal electron relaxation.

1. Introduction

Metal nanoparticles have attracted much attention because of their unique electronic and optical properties arising from reduced dimensionality and high surface-to-volume ratio.¹ Especially, gold nanoparticles exhibit a strong surface plasmon band, which originates from coherent collective electron oscillations coupled through the surface to the applied electromagnetic field. With consideration of high-order multipole terms and electron-surface scattering in nanoparticles, the spectral bandwidth, as well as the resonance frequency of the surface plasmon oscillation, has been investigated as a function of nanoparticle size.² Moreover, the dephasing time of surface plasmon was found to be around 8 fs from the near-field transmission spectra of a single gold nanoparticle.³

Because the surface plasmon band is very sensitive to the electron thermal motions and the lattice temperature, the thermalization dynamics in gold nanoparticles have been investigated by monitoring the bleach recovery of the collective electron oscillations in femtosecond pump-probe experiments.^{4–6} In the presence of hot electrons produced under the strong pump irradiation, a spectrally broader surface plasmon absorption is induced by the probe beam, because thermal motions of hot electrons increase the dephasing time of the surface plasmons. Consequently, the surface plasmon is bleached with two photoinduced absorption bands at low- and high-energy sides of the bleaching band.⁴ The electrons under ultrashort pulse excitation exist in nonequilibrium condition with the lattice (i.e., non-Fermi distribution). The electron thermalization process occurs internally through electron-electron collisions and externally through electron-phonon coupling. According to the transient absorption experiments,^{5,6} the thermal relaxation of hot electron gas into Fermi distribution via electron-electron

interactions takes as long as 0.5 ps in contrast with the assumption that the interactions would be even faster because of high concentration of electrons in metals.⁷ Therefore, electron-electron relaxation overlaps temporarily with the onset of electron-phonon relaxation, which occurs on the time scale of a few picoseconds. As a consequence, the two relaxation processes cannot be separated as expected from the two-temperature model (TTM).^{8,9} Because the lattice still heats electrons during the interactions between nanocrystals and embedding material, the time constant for phonon-phonon interactions has been also found to be ~ 100 ps from the bleach recovery of the surface plasmon band.^{1,4}

Although many investigations have been done on the surface plasmon and its bleaching dynamics, studies on the photoluminescence (PL) from gold nanoparticles are scarce. Wilcoxon et al.¹⁰ have recently reported the first observation of PL spectra from small gold nanoparticles, ~ 5 nm. In this work, the nanoparticles show quite high quantum efficiency ($\sim 10^{-4}$ – 10^{-5}), compared with gold films ($\sim 10^{-10}$). A relatively strong PL is considered to arise from an electrostatic enhancement mechanism, analogous to that in surface-enhanced Raman scattering (SERS). The ~ 5 nm nanocrystals exhibit the PL at 2.82 eV (440 nm) with photoexcitation at 5.39 eV (230 nm). In small gold nanoparticles, the electrons excited by the photons are free carriers. The interband transition from the d band to the Fermi level requires 2.4 eV of energy in gold. Because the 400 nm excitation exceeds the interband energy, it is possible that electronic transition from d band to conduction band occurs in addition to the intraband transition.¹¹ However, it is not reasonable to assign the light emission as originating from electron-hole pair recombination in the case of relatively large gold nanoparticles, because electrons in relatively large nanoparticles should be treated as Fermi electrons. Very recently,

the ultrafast (70 fs) enhanced light emission from gold–dendrimer nanocomposites was observed by the fluorescence up-conversion technique.¹² Thus, dendrimer plays a key role in the excitation dynamics of these nanocomposites serving as nonradiative relaxation channels. The fast nonradiative process could involve the coupling of the metal nanocomposites to the thermal reservoir of the host dendrimer, as well as the interaction of the emission dipole moment of the surface plasmon with that of the host dendrimer. Because the emission decay was much faster than the phonon coupling process with a characteristic time constant of a few picoseconds, it was suggested that electron–phonon interaction is not likely to contribute to the emission decay for gold metal–dendrimer nanocomposites. Instead, the emission process was suggested to be due to electron–electron and electron–surface scattering processes. Nevertheless, PL has not been observed for bare gold nanoparticles larger than ~ 5 nm even though we used the same method and reagents for the synthesis of large particles as for the 5-nm gold particle.

In the present work, we report the first observation of a weak light emission from bare gold nanoparticles of large size (~ 25 nm). The emission spectra show features similar to the surface plasmon resonance band in terms of its position and spectral width. To gain further insight into the dynamics of gold nanoparticles, it is relevant to monitor the bleach recovery of the plasmon absorption band and the emission decay simultaneously under the same experimental condition.

2. Experimental Section

The gold nanoparticles employed in our experiment were prepared by citrate reduction.¹³ In detail, 10 mL of gold chloride trihydrate solution containing 5 mg of Au was added to 85 mL of water (>18 M Ω) in a round-bottom flask with vigorous stirring. Then, 5 mL of 1% sodium citrate solution was added rapidly at the stage of boiling. The average diameter has been estimated to be ~ 25 nm from TEM image. The emission spectra from the gold nanocrystals have been measured by a cw Ar-ion laser and a 1-m double monochromator equipped with two 1800 grooves/mm gratings. To minimize the reabsorption of emission, the nanoparticle colloid solution was flowed through a 0.5 mm glass tube.

To measure the emission dynamics, the excitation pulses were generated by frequency doubling of a regeneratively amplified mode-locked Ti:sapphire laser (800 nm, 100 fs, and 1 kHz). The residual IR and fluorescence pulses were focused into another 1-mm β -BBO crystal to gate the up-conversion with a control of time delay. The up-converted signal was dispersed by a 0.3-m monochromator and then measured by a photomultiplier tube. The cross correlation between the excitation and the gate pulses is shown in Figure 2, from which the full width at half-maximum (fwhm) was estimated to be ~ 250 fs. The time resolution of ~ 100 fs was obtained by the deconvolution of the emission decay profiles with the cross correlation function with ~ 250 fs in fwhm.

The femtosecond transient absorption change of the surface plasmon band has been also observed by using the same excitation laser system. After probing the OD change of the gold nanoparticles photoexcited at 3.1 eV (400 nm), the delayed continuum pulses passed through a band-pass filter centered at 530 nm with 10-nm bandwidth.¹⁴ In the fluorescence up-conversion and transient absorption experiments, the colloidal gold nanoparticles were flowed in a 2-mm quartz cell and checked for the absence of any noticeable changes due to photodegradation.

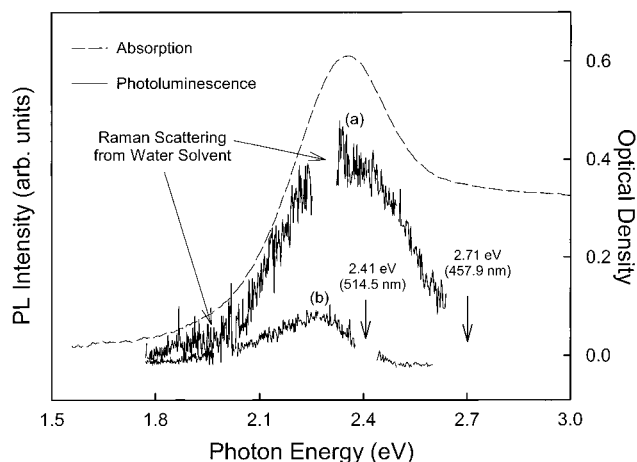


Figure 1. Linear absorption and PL spectra of gold nanoparticles ($d = 25$ nm). The maximum of the surface plasmon band is at 2.36 eV (526 nm). The PL spectra have been observed by photoexciting the nanocrystals at 2.41 (514.5) and 2.71 eV (457.9 nm). The discontinuities in the PL spectra are caused by the removal of the strong Raman scattering from the water solvent.

3. Results

The surface plasmon band (dotted line) and emission spectra (solid line) with photoexcitation at 2.71 eV from the gold nanocrystals are shown in Figure 1, from which the strong Raman band from water solvent was removed. The emission becomes weaker in the case of photoexcitation at 2.41 eV without a change in its spectral shape. To gain further insight into the electron–hole recombination in gold nanoparticles, the emission decay dynamics has been also investigated by using the femtosecond fluorescence up-conversion technique (Figure 2). Inset a shows the emission decay profiles probed at three different photon energies of 2.53, 2.34, and 2.14 eV (490, 530, and 580 nm). All of the profiles show nearly the same dynamics, in contrast with the intraband relaxation in semiconductor nanocrystals in which the decay dynamics at high photon energy is coincident with the build-up dynamics at low photon energy.¹⁵ The independence of the probe photon energy suggests that the emission process occurs almost instantaneously with thermalization of electrons above the Fermi level. Furthermore, the decay dynamics probed at 2.34 eV, at which the emission maximum is located (Figure 2), becomes significantly slower with increasing intensity. Inset b shows the temporal profiles in normalized logarithmic scale, from which the dependence on the excitation intensity is more clearly seen. The emission decay profiles exhibit also a slightly nonexponential feature, especially when the nanocrystals are photoexcited with high-intensity laser pulses.

Because the emission band overlaps spectrally with the surface plasmon oscillation, it is possible to compare the emission decay directly with the bleaching dynamics observed by transient absorption experiment (Figure 3). The emission decay dynamics including intensity dependence is similar to the bleaching recovery of the surface plasmon band, which follows the electron thermalization dynamics. The only difference is the diminishment of the long-lived component of phonon–phonon interaction in the emission decay profiles. The experimentally measured electron–phonon relaxation time increases with increasing electron temperature and hence pumping power. As illustrated in Figure 2, the temporal profiles of the plasmon bleach recovery become slower for nanoparticles monitored at 530 nm after photoexcitation with 400 nm femtosecond pulses increasing pump power. The normalized profiles in logarithmic

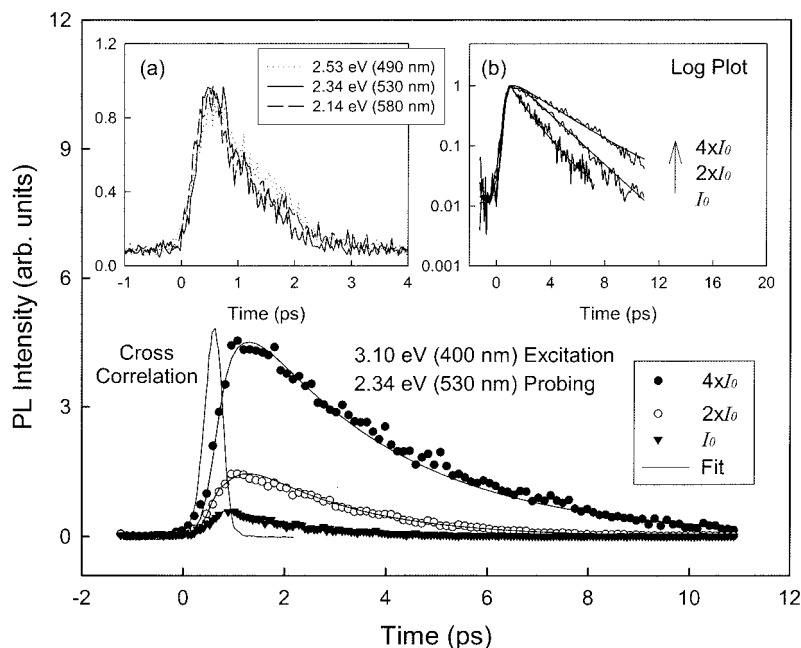


Figure 2. The PL decay profiles are measured by using femtosecond fluorescence up-conversion with varying excitation intensity ($I_0 = 15 \mu\text{J}/\text{cm}^2$). The decay profiles are well described by eq 1 with $\tau_{ee} = 0.3\text{--}0.4$ ps and $\tau_{ep} = 1.5$, 2.1, and 3.0 ps in the order of increasing intensity. Inset a exhibits three decay profiles probed at 2.53 (490), 2.34 (530), and 2.14 eV (580 nm) when the gold nanoparticles are excited with minimum intensity. Inset b shows the intensity dependence of the PL decay profiles in normalized logarithmic scale.

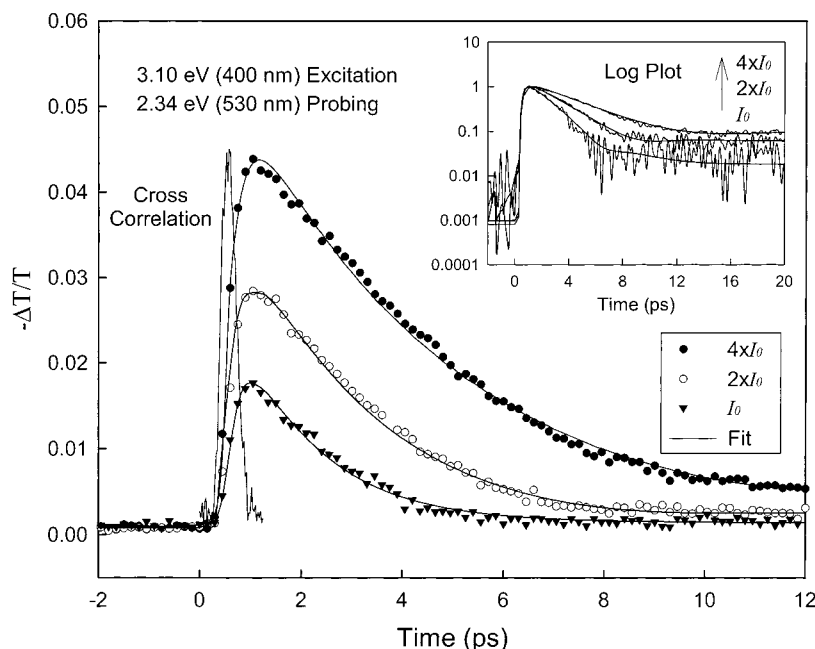


Figure 3. The bleaching recovery profiles of the surface plasmon band in gold nanoparticles photoexcited at various intensities ($I_0 = 30 \mu\text{J}/\text{cm}^2$). The bleach recovery profiles are well described by eq 1 with $\tau_{ee} = 0.3\text{--}0.4$ ps and $\tau_{ep} = 1.6$, 2.0, and 3.2 ps in the order of increasing intensity. The inset shows the intensity dependence of the bleach recovery profiles in normalized logarithmic scale.

scale in the inset show more clearly a long-lived component with a lifetime of ~ 100 ps, which was not observed in the fluorescence up-conversion measurement.

4. Discussion

Recently, Link et al.⁶ have also observed a nonexponential bleach recovery of the surface plasmon band in ~ 22 nm gold nanoparticles excited at 1.97 and 1.55 eV (630 and 800 nm) arising from the comparable time scale between electron–electron and electron–phonon interactions. When the nanocrystals are excited at 3.10 eV (400 nm), however, the temporal

profiles follow an exponential fit. Considering that the photoexcitation at 3.10 eV induces interband transitions, it has been suggested that the nonexponential feature would be obscured by a faster electron–electron scattering due to a greater perturbation of the electron gas in the interband transitions.¹ In contrast, the effect of electron–electron interactions has been observed in the bleach recovery of the surface plasmon band and more clearly in the emission decay, although the gold nanocrystals of nearly the same size (25 nm) are excited at the same photon energy. On the basis of the assumption that the contribution from the nonthermal electron gas is proportional

to its integrated energy density, the electron–electron interaction can be considered in the rate equation derived by modifying the two-temperature model.^{1,6,8} According to this model, the bleach recovery can be described by the following equation:

$$A(t) = A_{\text{NT}} \exp(-(t - t_0)/\tau_{\text{NT}}) + A_{\text{T}} \exp(-(t - t_0)/\tau_{\text{ep}}) \{1 - \exp(-(t - t_0)/\tau_{\text{ee}})\} \quad (1)$$

where $A(t)$ is the magnitude of the absorption change at a given time t with NT and T standing for the nonthermal and thermalized processes, respectively. The electron–electron and electron–phonon time constants are described by τ_{ee} and τ_{ep} , respectively, while

$$1/\tau_{\text{NT}} = 1/\tau_{\text{ee}} + 1/\tau_{\text{ep}} \quad (2)$$

By applying eq 1 to the bleach recovery dynamics of the surface plasmon band, the time constants of electron–electron and electron–phonon interactions have been estimated to be in the range of 0.3–0.4 and 1.6–3.3 ps, respectively, depending on excitation intensity. The electron–electron interaction times are in a good agreement with the reported values of 0.4–0.5 ps in the 22 nm nanocrystals in which only intraband transitions were induced.⁶ Assuming that the emission decay can be also described by eq 1, the observed emission profiles give the time constants of 0.3–0.4 and 1.5–3.0 ps for electron–electron and electron–phonon interactions. In addition, we also observed a weak contribution of the phonon–phonon interaction with the time constant of ~ 100 ps (Figure 3). Its amplitude is linearly increased with the incident power, which is consistent with the previous observations.¹ However, we could not observe a similar long-lived emission in the fluorescence up-conversion as shown in Figure 2, which might be due to the relatively lower excitation intensity as compared with transient absorption measurement and the low sensitivity of the fluorescence up-conversion measurement based on frequency mixing technique. Taking into account the fact that the excitation intensity of the fluorescence up-conversion experiments was lower than that for the bleaching recovery measurements, the obtained time constants are largely consistent with each other. It is to be noted that the phonon–phonon interactions occurring on the time scale of ~ 100 ps do not affect much the time constants and amplitudes for the electron–electron scattering and electron–phonon interactions, because the time constants for the phonon–phonon interactions are much larger than those of the other processes. The coincidence between the emission dynamics and the bleach recovery indicates that the light emission dynamics occurs simultaneously with the electron thermalization. If the light emission that we observed is the PL emission from the recombination processes between sp electrons and d band holes, the PL dynamics should be described in a different manner from the bleaching recovery of the surface plasmon band. Electrons are excited above the Fermi level of a dense Fermi sea, whereas holes are created in an empty band of totally different (relatively smooth) parabolicity. The hole dynamics is related to how quickly holes scatter from the d band to the sp bands, and thus, it is not thermalization dynamics—both thermalized and unthermalized states can be involved in the PL process. The created holes, if any, should have different hole–phonon interactions due to different masses from electrons. The different band structures between d and sp bands should also provide different energy transfer between holes/electrons and phonons. Because the PL line shape is contributed by the joint density of states multiplied by the occupancy of the d band states involved in the transition, the broad transition comes from the variation in

the sp final state energy corresponding to a wide wave vector distribution in the d band. Thus, it is more likely that the PL spectral shape does not exactly follow the surface plasmon band in its position and spectral shape. As a consequence, the light emission that we observed from bare gold nanoparticles seems to be a contribution from the conversion of surface plasmons to light energy arising from the interactions with the surface plasmon through the surface. This efficiency seems to be very low for larger particles (~ 25 nm) because the surface plasmon band shifts to higher energy with an increase in its intensity and the electrostatic enhancement starts to play a role in PL especially in smaller ($d < 5$ nm) particles. It is unlikely that the particles reradiate the same energy light directly at the surface plasmon frequency,¹⁶ because the PL temporal profiles observed in this work exhibit excitation density dependence corresponding to electron–phonon and electron–electron interactions.

5. Conclusions

We have observed, for the first time to our knowledge, the light emission spectrum and its decay profiles of relatively large gold nanoparticles (~ 25 nm). The emission band at 2.34 eV (530 nm) has been assigned to the light energy conversion arising from interactions between surface plasmons and incident photons rather than photoluminescence arising from recombination processes between sp band Fermi electrons and d band holes. The emission dynamics of bare gold nanoparticles observed by femtosecond fluorescence up-conversion technique closely follow the electron thermalization dynamics, which has been independently found from the bleaching recovery of the surface plasmon band. Therefore, it is concluded that the light emission from bare gold nanoparticles is attributable to surface plasmons based on the similarities in its decay dynamics and spectral shape to the surface plasmon band.

Acknowledgment. This work was supported by the National Creative Research Initiatives Program of the Ministry of Science and Technology of Korea.

References and Notes

- (1) Link, S.; El-Sayed, M. A. *J. Phys. Chem. B* **1999**, *103*, 8410.
- (2) Link, S.; El-Sayed, M. A. *J. Phys. Chem. B* **1999**, *103*, 4212.
- (3) Klar, T.; Perner, M.; Grosse, S.; von Plessen, G.; Spirk, W.; Feldmann, J. *Phys. Rev. Lett.* **1998**, *80*, 4249.
- (4) Ahmadi, T. S.; Logunov, S. L.; El-Sayed, M. A. *J. Phys. Chem.* **1996**, *100*, 8053.
- (5) Logunov, S. L.; El-Sayed, M. A.; Khoury, J. T.; Whetten, R. L. *J. Phys. Chem. B* **1997**, *101*, 3713.
- (6) Link, S.; Burda, C.; Wang, Z. L.; El-Sayed, M. A. *J. Chem. Phys.* **1999**, *111*, 1255.
- (7) Sun, C.-K.; Vallée, F.; Acioli, L. H.; Ippen, E. P.; Fujimoto, J. G. *Phys. Rev. B* **1993**, *48*, 12365.
- (8) Sun, C.-K.; Vallée, F.; Acioli, L. H.; Ippen, E. P.; Fujimoto, J. G. *Phys. Rev. B* **1994**, *50*, 15337.
- (9) Groeneveld, R. H.; Sprik, R.; Lagendijk, A. *Phys. Rev. B* **1995**, *51*, 11433.
- (10) Wilcoxon, J. P.; Martin, J. E.; Parsapour, F.; Wiedenman, B.; Kelley, D. F. *J. Chem. Phys.* **1998**, *108*, 9137.
- (11) Cracknell, A. P. In *Numerical Data and Functional Relationships in Science and Technology*; Hellwege, K.-H., Olsen, J. L., Eds.; Landolt-Börnstein New Series Group III; Springer-Verlag: Berlin, 1984; Vol. 13C, p 48.
- (12) Varnavski, O.; Ispasoiu, R. G.; Balogh, L.; Tomalia, D.; Goodson, T., III. *J. Chem. Phys.* **2001**, *114*, 1962.
- (13) Turkevich, J.; Garton, G.; Stevenson, P. C.; Hillier, J. *Discuss. Faraday Soc.* **1951**, *11*, 55.
- (14) Klimov, V. I.; McBranch, D. W. *Opt. Lett.* **1998**, *23*, 277.
- (15) Klimov, V. I.; Bolivar, P. H.; Kurz, H. *Phys. Rev. B* **1996**, *53*, 1463.
- (16) Kokkinakis, Th.; Alexopoulos, K. *Phys. Rev. Lett.* **1972**, *28*, 1632.